

## Octupole Softness of Superdeformed $^{194}\text{Pb}$

P. Bonche,<sup>(a)</sup> S. J. Krieger, and M. S. Weiss

*Department of Physics, Lawrence Livermore National Laboratory, Livermore, California 94550*

J. Dobaczewski

*Institute of Theoretical Physics, Warsaw University, Hoza 69, PL-00681 Warsaw, Poland*

H. Flocard

*Division de Physique Théorique, Institut de Physique Nucléaire, 91406 Orsay CEDEX, France*

P.-H. Heenen

*Service de Physique Nucléaire Théorique, Université Libre de Bruxelles, CP229, 1050 Bruxelles, Belgium*

(Received 14 November 1990)

Using parity projection and the generator-coordinate method we investigate the left-right-asymmetric softness of the superdeformed minimum of  $^{194}\text{Pb}$ . The collective wave functions exhibit large octupole dispersions. Our calculation suggests that above the ground-state superdeformed band there should exist a negative-parity band of similar quadrupole deformation with an excitation energy close to 2 MeV.

PACS numbers: 21.10.Re, 21.60.Jz, 27.80.+w

The octupole degree of freedom is known to be important for the description of fission of actinide elements. In many nuclei the fission path is unstable against octupole deformation when the quadrupole deformation becomes very large.<sup>1-3</sup> Several theoretical analyses<sup>4-10</sup> have also suggested an octupole softness of the superdeformed (SD) minima found in the energy surfaces of light Pb and Hg isotopes which have been associated with recently discovered SD bands.<sup>10-20</sup> Moreover, several excited SD bands observed<sup>10</sup> in  $^{193}\text{Hg}$  have been considered as providing evidence for the presence of octupole correlations in the SD states. As of today, the position of these bands relative to the yrast configuration has not been measured. Further, neither does a theoretical estimate of their excitation energy exist. This is attempted in this Letter, in which we construct the octupole collective wave functions of the intrinsic states of both the positive- and negative-parity SD states.

In what follows we concentrate our analysis on the nucleus  $^{194}\text{Pb}$  where SD bands have also been found.<sup>16,17</sup> It belongs to the region of superdeformation centered around the "magic" SD nucleus  $^{192}\text{Hg}$ . The calculations presented here are based on the Hartree-Fock+BCS (HFBCS) theory to construct the collective space, and on the generator-coordinate method (GCM) to describe the dynamics within this space. In both methods we use the same SkM\* Skyrme effective Hamiltonian.<sup>21</sup> These theoretical ingredients have already been employed in a previous discussion of the SD states in the  $A=190$  region and have been presented in detail in Refs. 22-24.

Our choice of the nucleus  $^{194}\text{Pb}$  is motivated by the fact that triaxial quadrupole deformation ( $\gamma \neq 0$ ) plays a smaller role in this nucleus than in the mercury isotopes. This allows us to restrict the analysis to axial shapes of

$^{194}\text{Pb}$  only. As seen in the bottom part of Fig. 1, the HFBCS ground state of  $^{194}\text{Pb}$  is spherical. The deformation-energy curve was constructed with a constraint on the axial quadrupole moment for values of  $q_2 = \langle \hat{Q}_2 \rangle = \langle 2z^2 - x^2 - y^2 \rangle$  ranging from -34 to 66 b. In addition to the spherical ground state, one finds a SD minimum at  $q_2 \approx 46$  b with an excitation energy of about 4.7 MeV. The oblate and prolate minima which were observed at small deformations in the curves of the Hg isotopes<sup>24</sup> appear only as shoulders or inflections on the deformation curve at  $q_2 \approx 10$  b. The barrier between the SD and the main well is located at 34 b, and is about 1.3 MeV above the SD minimum. The properties of this minimum in  $^{194}\text{Pb}$  are therefore similar to those found<sup>24</sup> in  $^{194}\text{Hg}$ , except for the excitation energy which is higher in the latter nucleus. This suggests the SD in  $^{194}\text{Hg}$  to depopulate at a higher angular momentum than in  $^{194}\text{Pb}$ , which agrees with the current experimental interpretation.<sup>16,17</sup>

Following the same procedure as in Ref. 23 we have solved the GCM equations using the average value of quadrupole moment  $q_2$  as the collective variable. Based on our previous experience, the mesh size  $\Delta q_2$  used in the numerical solution of the Hill-Wheeler equation has been taken equal to 4 b. We have also included a constraint on the neutron and proton number as discussed in Ref. 23.

The GCM spectrum is reported in the bottom part of Fig. 1 where each state is indicated by a short horizontal bar drawn at the corresponding energy and a dot at the average quadrupole moment. The lowest state is spherical and 1.5 MeV below the HFBCS minimum. As in the Hg isotopes, we find that compared to the mean-field predictions, the energy of the SD GCM state is lowered

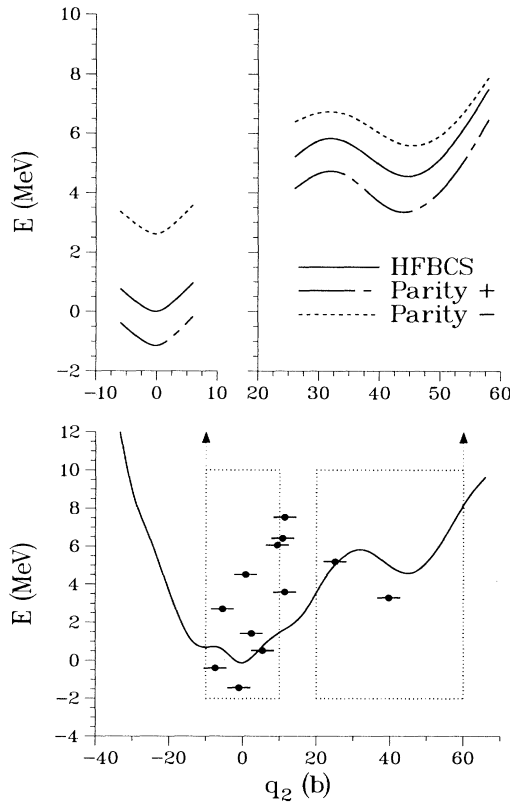


FIG. 1. HFBCS deformation-energy curve of  $^{194}\text{Pb}$  as function of the quadrupole deformation  $q_2$  shown as solid line (bottom). The energies and quadrupole moments of GCM states are shown as short horizontal bars. The top part shows a magnification of a region including the barrier and the SD minimum. This part also shows the evolution as a function of  $q_2$  of the energy of the positive- (long-dashed line) and negative- (dashed line) parity-projected states. The left part gives the same information for the energies of the HFBCS ground state and the lowest positive- and lowest negative-parity-projected states at  $q_2 = 0$ .

by about the same amount (1.15 MeV), and that its quadrupole moment is reduced ( $q_2 \approx 40$  b).

We turn now to the analysis of the octupole deformation properties. To construct octupole-deformation-energy curves for fixed values of the quadrupole moment we have introduced an additional constraint on the mean square of the scalar constructed with the average values of components of the octupole moment operator:  $q_3 = (\langle \hat{Q}_3^2 \rangle)^{1/2}$ , with  $\langle \hat{Q}_3^2 \rangle = \sum_{\mu=-3}^3 (-1)^\mu \langle \hat{Q}_{3\mu} \rangle \langle \hat{Q}_{3-\mu} \rangle$  and  $\hat{Q}_{3\mu} = r^3 Y_{3\mu}(\theta, \phi)$ . This choice has the advantage of not precluding nonaxial octupole deformations. However, since we enforce a symmetry of the HFBCS states with respect to the  $x$  and  $y$  planes, the contributions of the  $\mu = \pm 1$  and  $\pm 3$  components are suppressed. In addition, the axial constraint along the  $z$  axis generated by the operator  $\hat{Q}_2$  almost eliminates all of the  $\mu = \pm 2$

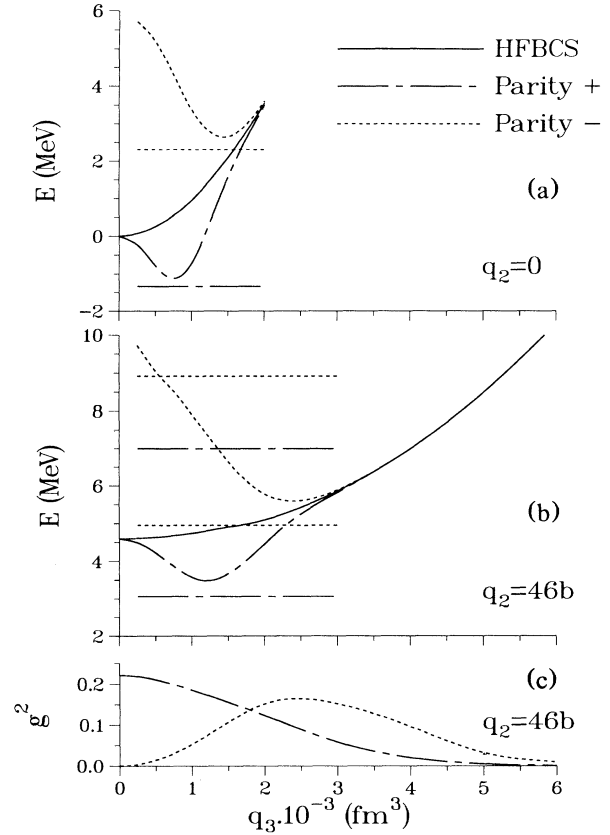


FIG. 2. Octupole-deformation properties of  $^{194}\text{Pb}$  at (a) the ground state ( $q_2 = 0$ ) and (b) the SD minimum ( $q_2 = 46$  b). The solid lines show the HFBCS energies as a function of the octupole moment  $q_3$ . The long-dashed (dashed) line gives the energies of the positive (negative) parity projected at a given  $q_3$ . The long-dashed and dashed horizontal lines indicate the energies of the GCM positive- and negative-parity states. (c) The probability distributions of the lowest GCM collective wave functions of both parities at the quadrupole deformation of the SD minimum.

components. Therefore, in the present work, the constraint on  $(\langle \hat{Q}_3^2 \rangle)^{1/2}$  turns out to be equivalent to one on  $\langle \hat{Q}_{30} \rangle$  for all practical purposes.<sup>25</sup>

The solid line in Fig. 2(a) shows the HFBCS energy as a function of  $q_3$  for the zero value of the quadrupole moment ( $q_2 = 0$ ). This curve illustrates the octupole stiffness at the spherical minimum. For each value of  $q_3$  we have projected states with good parity out of the HFBCS solution, according to the method exposed in Refs. 26 and 27. The energies of projected states are shown in Fig. 2(a) as long-dashed and dashed lines for positive and negative parity, respectively. Projecting the HFBCS state with an octupole moment  $q_3 = 750 \text{ fm}^3$  leads to a 1.05-MeV energy lowering with respect to the HFBCS minimum. The lowest point on the negative-parity curve lies 3.8 MeV above the positive minimum,

and corresponds to  $q_3 = 1400 \text{ fm}^3$ .

The excitation of about 6 MeV of the negative- relative to the positive-parity-projected curve at  $q_3 = 0$  is, as expected, of the order of magnitude of the energy difference between major shells. On the other hand, the 3.8-MeV difference between energies of negative and positive minima should be indicative of the energy of a coherent octupole vibration. This value is somewhat larger than the expected excitation energy of the lowest  $3^-$  state. Similar calculations<sup>26,28</sup> in nuclei of the thorium region where the existence of stable octupole deformations is well established have given fair agreement with observed positive-negative bandhead energy differences.<sup>29,30</sup>

It is important to keep in mind that the  $q_3$  values of the minima of parity-projected curves should not be interpreted as static octupole deformations, and that the value of 1.05 MeV mentioned above does not represent a barrier between symmetric and asymmetric configurations. Once parity projection has been effected, the resulting multideterminant wave functions include correlations beyond the mean field, and both positive- and negative-parity-projected states have a zero expectation value of  $\hat{Q}_{30}$ . In our opinion, the correct interpretation is that the  $q_3$  values at the minima of parity-projected curves are only indicative of the amounts of octupole fluctuations that are present in the optimal intrinsic state pertaining either to the positive- or to the negative-parity bands.

We now perform the same type of analysis for the fixed quadrupole deformation  $q_2 = 46 \text{ b}$  of the SD minimum of the energy curve displayed in Fig. 1. The results are shown in Fig. 2(b). The HFBCS curve (solid line) shows that even though the SD state remains stable against octupole excitation, it is much softer than that at  $q_2 = 0$ . In order to obtain an energy increase of 1 MeV,  $q_3$  must reach  $2750 \text{ fm}^3$  at the SD shape, while the same excitation requires only  $q_3 = 1000 \text{ fm}^3$  at the spherical minimum. The positive- and negative-parity-projected energy curves display a behavior similar to that seen in Fig. 2(a). The three curves merge above  $q_3 \sim 3000 \text{ fm}^3$  when the overlap between the  $\pm q_3$  partners vanishes. The positive-parity minimum is about 1.15 MeV below the HFBCS SD minimum. This value is similar to that obtained at  $q_2 = 0$  but the minimum is obtained from an intrinsic state with a much larger value of  $q_3$  ( $1250 \text{ fm}^3$ ). Similarly, the minimum of the negative-parity curve occurs at  $q_3 = 2500 \text{ fm}^3$  instead of  $q_3 = 1400 \text{ fm}^3$  at  $q_2 = 0$ . In addition it lies only 2.1 MeV above the parity minimum. This value, which is almost a half of that at  $q_2 = 0$ , indicates the increased octupole softness near the SD minimum, and provides us with a first estimate of the excitation energy of a possible octupole collective SD band of negative parity.

Since the HFBCS curve is rather flat as a function of  $q_3$  one should expect that many configurations with dif-

ferent  $q_3$  values will contribute to the octupole collective function. This was tested in GCM calculations using  $q_3$  as the collective variable. To discretize the GCM problem we have used the mesh size  $\Delta q_3 = 1000 \text{ fm}^3$ . We adopted this value after checking that it was smaller than the  $q_3$  width of the overlap kernel entering the Hill-Wheeler equation. Indeed, we found that this width was approximately equal to  $1750 \text{ fm}^3$  over a range of  $q_3$  values between 0 and  $6000 \text{ fm}^3$ . As for the case of quadrupole GCM, we have added a constraint on neutron and proton numbers to ensure that final states have the correct  $N$  and  $Z$  values.

As expected, the lowest GCM state has a positive parity. Its energy is 1.53 MeV below that of the HFBCS SD minimum, and is presented as the lowest long-dashed horizontal line in Fig. 2(b). This value is larger than the 1.15 MeV lowering due to the quadrupole correlations (see SD GCM state at  $q_2 \approx 40 \text{ b}$  in the bottom part of Fig. 1). Therefore, the effect of the octupole deformation on the energy of the shape isomer turns out to be more important than the quadrupole one. The energy of the first negative-parity excited state (second GCM state) is indicated by the lowest dashed line in Fig. 2(b) and is only 1.9 MeV above that of the positive-parity GCM state. The energies of two more GCM octupole states are also indicated in Fig. 2(b) by long-dashed and dashed lines according to their parities.

The GCM probability densities for the lowest states of both parities are presented in Fig. 2(c). One sees that both distributions are rather wide, indicating that many different configurations enter the GCM collective states. On the other hand, the fact that the GCM octupole excitation energy (1.9 MeV) is almost the same as that obtained by a simple parity projection (2.1 MeV) indicates that positive- and negative-parity states are affected similarly by the configuration mixing. One notes also that the maximum of the distribution for the negative-parity state occurs at  $2500 \text{ fm}^3$ , namely, the  $q_3$  value at the minimum of the negative-parity-projected energy curve.

The energies resulting from the octupole GCM calculations at  $q_2 = 0$  are presented in Fig. 2(a). They confirm that conclusions drawn from parity-projection calculations are not significantly altered by the GCM calculation. One can also remark that the energy gain due to octupole correlations (1.35 MeV) is of the order of magnitude of that due to quadrupole correlations (1.5 MeV).

So far we have only performed octupole GCM calculations for fixed value of  $q_2$ . Since the effect of octupole and quadrupole correlations appears to be of similar magnitude, a two-dimensional ( $q_2$ - $q_3$ ) GCM calculation, which would allow an investigation of the coupling of both modes, appears very desirable. It requires, however, a much larger numerical effort and has not yet been done. On the other hand, we have seen that both at

$q_2=0$  and 46 b there is good agreement between results derived from GCM and from parity projection. We have therefore decided to investigate the stability versus quadrupole motion of octupole SD bands by means of the latter simpler method.

The results are shown in the upper part of Fig. 1 for values of  $q_2$  ranging from 26 to 60 b. Except for overall energy shifts, the HFBCS and parity-projected curves are very similar. The barrier and the SD well have the same quadrupole deformations. The depth of the second well is also roughly the same ( $\sim 1.3$  MeV). Therefore, one can expect that the  $q_2$  localization of the even and odd isomeric collective states will be identical to that predicted by calculations like those of Ref. 24 which do not take into account the octupole degrees of freedom. The energy difference between the ground and isomeric states is smaller for the odd GCM state than for the even one, so the depopulation of the negative-parity octupole SD band via direct  $E2$  transitions to states in the first well may be less effective than for the even SD band. At first sight this may allow the former band to reach a lower angular momentum. However, a quantitative prediction will have to include the influence of  $E1$  transitions whether they are of a statistical nature towards states of the main well or collective towards the positive-parity SD band.

This work presents the first dynamical analysis of the implications of the octupole softness expected for the SD states of the Hg region of the mass table. From our findings, one may expect that, in addition to the even SD shape isomer, there will exist an odd one on which may be built another superdeformed rotational band.

During the completion of this work, one of the authors (P.B.) has benefited from many valuable discussions with J. F. Berger and D. Gogny. This work was supported in part by the U.S. Department of Energy under Engineering Contract No. NW 7405-ENG-48 and in part by the Polish Ministry of National Education under Contract No. CPBP 01.09. Division de Physique Théorique is a unité de recherches des Universités Paris XI et Paris VI associée au CNRS. P.-H.H. is directeur de recherches Fonds National de la Recherche Scientifique.

(a)Permanent address: Service de Physique Théorique, Direction des Sciences de la Matière du Commissariat à l'Energie Atomique, F-91191 Gif-sur-Yvette CEDEX, France.

<sup>1</sup>J. F. Berger, M. Girod, and D. Gogny, Nucl. Phys. **A502**, 85c (1990).

<sup>2</sup>J. Blons, Nucl. Phys. **A502**, 121c (1990).

<sup>3</sup>J. R. Nix, Nucl. Phys. **A502**, 609c (1990).

<sup>4</sup>T. Bengtsson *et al.*, Phys. Scr. **24**, 200 (1981).

<sup>5</sup>J. Dudek, in *The Variety of Nuclear Shapes*, edited by J. D. Garrett *et al.* (World-Scientific, Singapore, 1987), p. 195.

<sup>6</sup>J. Höller and S. Åberg, Z. Phys. A **336**, 363 (1990).

<sup>7</sup>S. Mizutori, Y. R. Shimizu, and K. Matsuyanagi, in Proceedings of the International Conference on Nuclear Structure in the Nineties, Oak Ridge, April 1990, p. 28.

<sup>8</sup>S. Åberg, Nucl. Phys. A (to be published).

<sup>9</sup>J. Dudek, T. Werner, and Z. Szymański, Phys. Lett. **B 248**, 235 (1990).

<sup>10</sup>D. M. Cullen *et al.*, Phys. Rev. Lett. **65**, 1547 (1990).

<sup>11</sup>E. F. Moore *et al.*, Phys. Rev. Lett. **63**, 360 (1989).

<sup>12</sup>J. A. Becker *et al.*, Phys. Rev. C **41**, R9 (1990).

<sup>13</sup>D. Ye *et al.*, Phys. Rev. C **41**, R13 (1990).

<sup>14</sup>C. W. Beausang *et al.*, Z. Phys. A **335**, 325 (1990).

<sup>15</sup>E. A. Henry *et al.*, Z. Phys. A **335**, 361 (1990).

<sup>16</sup>M. J. Brinkman *et al.*, Z. Phys. A **336**, 115 (1990).

<sup>17</sup>K. Theine *et al.*, Z. Phys. A **336**, 113 (1990).

<sup>18</sup>F. Azaiez *et al.*, Z. Phys. A **336**, 243 (1990).

<sup>19</sup>M. P. Carpenter *et al.*, Phys. Lett. **B 240**, 44 (1990).

<sup>20</sup>M. A. Riley *et al.*, Nucl. Phys. **A512**, 178 (1990).

<sup>21</sup>J. Bartel *et al.*, Nucl. Phys. **A386**, 79 (1982).

<sup>22</sup>P. Bonche *et al.*, Nucl. Phys. **A500**, 308 (1989).

<sup>23</sup>P. Bonche *et al.*, Nucl. Phys. **A510**, 466 (1990).

<sup>24</sup>P. Bonche *et al.*, Nucl. Phys. A (to be published).

<sup>25</sup>At the spherical point, the first-order relation between the octupole moment  $q_3$  and the octupole Bohr deformation parameter  $\beta_3$  reads  $\beta_3 = 4\pi q_3 / 3AR_0^3$ , where  $R_0$  is the nuclear radius, i.e.,  $\beta_3 = q_3 / 16\,000 \text{ fm}^3$  for  $^{194}\text{Pb}$ . Taking into account the effect of quadrupole deformation ( $q_2 = 46 \text{ b}$ ) yields  $\beta_3 = q_3 / 27\,000 \text{ fm}^3$  at the SD minimum.

<sup>26</sup>P. Bonche, in *The Variety of Nuclear Shapes* (Ref. 5), p. 302.

<sup>27</sup>J. L. Egido and L. M. Robledo, Universidad Autónoma de Madrid Report No. FT/UAM-90-016, 1990 (to be published).

<sup>28</sup>P. Bonche *et al.*, Phys. Lett. **B 175**, 387 (1986).

<sup>29</sup>J. F. Shriner *et al.*, Phys. Rev. C **32**, 1888 (1985).

<sup>30</sup>P. Schüler *et al.*, Phys. Lett. **B 174**, 241 (1986).